chemosensors

MDPI

Article

A Reaction-Based Approach to Colorimetric Detection of Organic Analytes in Water Using a Chlorine-Containing Carbocyanine Dye and Hypochlorite

Anna V. Shik [1], Evgenii V. Skorobogatov [1], Ramil M. Akhmetov [1], Irina A. Doroshenko [1], Tatyana A. Podrugina [1], Gleb K. Sugakov [2] and Mikhail K. Beklemishev [1,*]

[1] Department of Chemistry, Lomonosov Moscow State University, 119991 Moscow, Russia; shik.1966@mail.ru (A.V.S.); skoregy@gmail.com (E.V.S.); ramil.akhmetov.2004@gmail.com (R.M.A.); doroshenkoiran@gmail.com (I.A.D.); podrugina@mail.ru (T.A.P.)

[2] Centre for Global and Strategic Studies, Institute for African Studies of the Russian Academy of Sciences, 123001 Moscow, Russia; g.sugakov@inafr.ru

* Correspondence: mkb@analyt.chem.msu.ru

Abstract: Water quality control employs techniques mostly targeting individual analytes; group detection is also practiced, but the choice of group methods is limited, which supports interest in developing such methods. We have examined the interaction of hypochlorite with a chlorine-containing heptamethine carbocyanine dye in the presence of 30 organic and inorganic model analytes that were found to induce diverse color changes in the system. The main supposed mechanisms are retardation of the dye oxidation with hypochlorite (presumably by scavenging chlorine radicals) and substitution of chlorine atom in the dye by the most nucleophilic analytes (amines, amino acids, proteins, DNA, phenol). The grass-green substitution product is more contrastingly visible against the dark-purple hypochlorite oxidation product of the dye than against the original emerald-green dye. The indicator reaction is monitored photographically for 10–40 min and the images are processed using principal component analysis (PCA) or linear discriminant analysis (LDA), allowing for data convolution for the complex color transitions. Nitrogen compounds are discriminated from the others, and more reactive analytes (tryptophan, cysteine, bovine serum albumin, and DNA) are detected in the presence of less reactive ones in natural water. The system is promising for the development of group assays for dissolved organic matter and the discrimination of water samples.

Keywords: color test; carbocyanines; hypochlorite; organic analytes; nitrogen compounds; machine learning; natural water; wastewater

Citation: Shik, A.V.; Skorobogatov, E.V.; Akhmetov, R.M.; Doroshenko, I.A.; Podrugina, T.A.; Sugakov, G.K.; Beklemishev, M.K. A Reaction-Based Approach to Colorimetric Detection of Organic Analytes in Water Using a Chlorine-Containing Carbocyanine Dye and Hypochlorite. *Chemosensors* **2024**, *12*, 224. https://doi.org/10.3390/chemosensors12110224

Received: 30 August 2024
Revised: 15 October 2024
Accepted: 25 October 2024
Published: 27 October 2024

1. Introduction

Control of water sources is critical to ensure the normal life of human communities. As of 2022, 2.2 billion people in the world did not have access to clean drinking water; the problem is most acute in developing countries, including Sub-Saharan Africa. Despite the efforts of international organizations and the adoption of the Sustainable Development Goals, aimed, among other things, at improving the state of water resources, no significant progress has been observed in recent years [1].

The analytical information on the organic matter dissolved in water is gained by advanced techniques such as high-resolution mass spectrometry, chromatography–mass spectrometry, and others [2]. However, the number of organic compounds in water is in the hundreds, which is difficult to monitor by techniques that determine individual components. This situation raises interest in molecular spectroscopy techniques (UV–Vis, fluorescence, infrared, and Raman spectroscopy) that provide information about groups of compounds [3]. Due to simple equipment and affordability, a number of indices and parameters have been developed to characterize organic matter-containing samples without

its prior separation into fractions: specific UV absorbance parameters ($SUVA_{280/365/436}$), absorption ratios at different wavelengths, such as E2/E3 (at 250/365 nm), the spectral slopes and slope ratios ($S_{275–295}/S_{350–400}$) are associated with the level of double bonds, molecular weight, aromaticity, polarity, humification and hydrophobicity of organic matter, prediction of lignin phenols, and hydrophobic/hydrophilic species content [4].

A number of group tests for organic compounds are based on chemical reactions with UV–vis and fluorimetric control. Examples of such assays are chemical oxygen demand determination by permanganate or dichromate oxidation [5], a ninhydrin test for amino compounds [6], a thiobarbituric acid-reactive compounds test (TBARS) [7], a test for thiols and disulfides [8], nitroaromatics and nitrates [9], and antioxidant capacity tests (ferric ion reducing antioxidant power (FRAP), cupric ion reducing antioxidant capacity (CUPRAC), 2,2-diphenyl-1-picrylhydrazyl (DPPH) radical scavenging, and others [9,10]). The existing tests still do not characterize the samples comprehensively due to the presence of unreactive components [11], which raises interest in developing assay methods for other groups of compounds, for example, thioamides [12].

Analytical characterization of complex samples such as natural waters or foods became more efficient with the development of sensor array techniques based on pattern recognition [13] in combination with machine learning data processing. Nevertheless, optical sensors for water quality control have been developed mostly for the detection of particular compounds and less frequently for integral parameters such as turbidity, chemical oxygen demand [14], or groups of analytes such as heavy metal ions [15,16], aromatic hydrocarbons [17], or organophosphorus pesticides [18]. Examples of the application of optical sensor arrays for the discrimination and determination of such groups of analytes as polyhydroxy compounds, flavonoids, sulfur compounds, organic acids, amines, amino acids, and saccharides mainly refer to model solutions [19]. Direct group assays of organic species by optical sensing arrays in real-world samples remains a challenge that requires more research.

Up to 60 compounds were found in most surface waters at low but measurable concentrations and recommended for water quality control (pharmaceuticals, fragrances, surfactants, biocides and plasticizers, disinfection by-products) [20]. Some of these and several other compounds can indicate discharges to water, for example, fecal sterols and bile acids can help detect animal or human wastewater, and the latter can be identified by artificial sweeteners [21]. Treated wastewater effluent can be recognized by benzaldehyde, benzonitrile, chlorobutanoic acid, and other compounds [22]. However, these markers do not account for a sudden release of a chemical not included in this list, increasing interest in methods that respond to the widest possible range of compounds.

An essential part of water treatment is disinfection using active halogen reagents (chlorine gas, hypochlorite, chloramine, etc.) with the formation of potentially harmful disinfection by-products (DBPs) [23], especially nitrogenous DBPs that are considered more toxic than the others [24]. Primary amino group-containing compounds (amines, amino acids, proteins, amino sugars), which are non-toxic themselves, are believed to be the main precursors of N-DBPs [25] and should be included among the model analytes.

As the socio-economic situation in many developing countries remains difficult, the possibility of applying new methods is closely related to their simplicity and low cost. The approach proposed in this article is aimed at the development of tests for the gross assessment of water quality rather than determining individual components, which avoids using multiple tests and can significantly decrease costs. It will be possible to develop methods, for example, to detect sudden discharges from industrial plants and to monitor the effects of floods on water bodies, as agricultural waste can enter rivers and lakes in large quantities. For example, in 2024 alone, floods in the East African region affected more than 600,000 people [26]. When the same water sources are regularly monitored, a database is built up, with which the current result of the analysis can be compared; therefore, field assay methods can contribute to a long-term solution for the water problem.

Earlier, we studied two types of processes of chlorine-containing heptamethine carbocyanine dyes: a hypochlorite oxidation reaction that was applied for the discrimination of natural water samples [27], and the substitution of chlorine atom that was used to determine isoniazid [28]. These indicator reactions feature multiple color transitions and near-IR fluorescence signals. An essential feature of the discrimination technique was the use of the kinetic factor by monitoring the optical signal over time with digital cameras, which expanded the set of data obtained from the reacting system.

In the present study, we observed a combination of these types of processes, when carbocyanine I (Scheme 1) was reacted with NaOCl in the presence of various model compounds. The purpose of this study was to explore the possibilities of the dye I–NaOCl system as an indicator reaction for the discrimination of individual low-molecular organic analytes belonging to different groups. It was necessary to reveal the effects of compounds of various classes on the course of the reaction, study the effects of the concentrations and co-presence of analytes, find out the feasibility of detecting analytes in the presence of natural water, and differentiating between natural and wastewater samples.

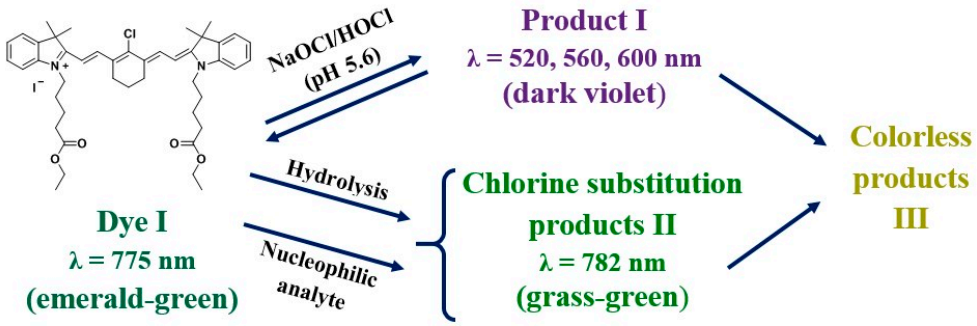

Scheme 1. Structure of carbocyanine dye I and main processes in the *dye–NaOCl–analyte* system. Absorption maxima of the dye and products are indicated.

2. Materials and Methods

2.1. Reagents and Water Samples

Carbocyanine dye I was synthesized by the authors according to a published protocol [29]; the spectral data for the dye are given in ESI. The dye was dissolved at 1 g/L in 96% ethanol (Bryntsalov-A, Moscow, Russia) and stored at 4 °C. Model proteins: lysozyme from chicken egg white, CAS No 12650–88-3, was from Sigma–Aldrich (St. Louis, MO, USA); bovine serum albumin (BSA), CAS No 9048–46-8, was from Sigma (Taufkirchen, Germany). DNA from salmon testes was supplied by Immunolex (Moscow, Russia) as 2.5% (*w*/*v*) aqueous solution (Derinat). Other model analytes were purchased from Sigma–Aldrich (St. Louis, MO, USA) and used as 5 mM aqueous solutions. Most experiments were conducted in 0.01 M acetate buffer solution (pH 5.6). Sodium hypochlorite (Aquatics, Moscow, Russia) was received as 2 M solution and diluted to 5 mM to receive working solution. Aqueous solutions were prepared using water treated in a Millipore water purification system (Millipore water). Natural water samples collected in central Russia and sewage water samples were kindly provided by the Analytical Center of Moscow University; the characteristics of the samples are listed in Tables S1 and S2 in ESI.

2.2. Instrumentation

Absorption spectra were measured using SF-102 spectrophotometer (Interfotofizika, Moscow, Russia) in 0.2 cm × 1.0 cm quartz cells (internal volume of 0.5 mL, optical path length of 1 cm); fluorescence spectra were obtained on a Fluorat-02 Panorama spectrofluorimeter (Lumex, St. Petersburg, Russia). Reactions were carried out in white 96-well fluorimetric plates (cat. No M-018, Sovtech, Berdsk, Russia). Absorbance/reflectance of the reaction mixtures in the plates was measured using Visualizer 2 (Camag, Muttenz, Switzerland), and near-IR fluorescence was detected with an in-house manufactured visualizer [30]

containing red LEDs (660 nm) as a light source (Minifermer, Moscow, Russia) and a Nikon D80 camera with a light filter to cut off light with wavelength under 700 nm.

2.3. Indicator Reaction Protocols and Data Processing

In a typical experiment, the following solutions were added to the wells of a fluorimetric plate: 30 μL of 0.1 M acetate buffer solution (pH 5.6), 30 μL of ethanol, 30 μL of the sample or solution of a model analyte (5 mM, if not stated otherwise), water up to 300 μL, 30 μL of 0.0025 M sodium hypochlorite, 30 μL of 0.1 g/L dye I. When the reaction was conducted in the presence of natural water, 120 μL of it was added to each well. The moment of adding the dye was taken as the reaction start, after which the reaction mixtures were photographed using visualizers. Typically, the images were captured at 1, 2, 3, 5, 7, 10, 15, 20, and 30 min after the start of the reaction (if not stated otherwise). The photographs were processed to obtain the average intensities of the RGB channels of the wells using software developed by the authors. The desktop application included a YOLO neural network model for object detection [31] and a post-processing algorithm with a graphical user interface written in Python. The neural network model was trained to detect wells in photographs of the plates. The program output the RGB channel intensity values to an MS Excel file. The RGB intensities were organized into data tables so that the rows corresponded to different wells of the plate (to be called observations), and the columns referred to different color channels (R, G, B) at different reaction times (i.e., 1 min,R; 1 min,G; 1 min,B; 3 min,R; 3 min,G; 3 min,B; etc.). The chemometric techniques used were principal component analysis (PCA) and linear discriminant analysis (LDA); XLSTAT add-on for Microsoft Excel (version 2016.02.28451, Lumivero, Denver, CO, USA) was used for PCA and LDA processing. PCA uses an unsupervised technique, in which the software is not informed about the division of the data into classes, so it is an objective approach to data convolution. When PCA could not adequately divide the data into the groups of interest, LDA was used; in this technique, the software is provided with information about the division of observations into classes, and its task is to discriminate these classes. In LDA, a validation procedure is possible, where the software randomly sets aside each 6th (in this work) observation (validation set) and builds a discrimination model using the remaining 83.3% of observations (training set). The observations from the validation set are then assigned to one or another class using the built model. The ratio of correctly assigned observations to the total number of observations in the validation set is called the discrimination accuracy (%), which characterizes the quality of discrimination.

3. Results and Discussion

3.1. Hydrolysis of Dye I

When an ethanol solution of carbocyanine I is diluted with an aqueous buffer, the emerald-green dye (λ_{max} = 780 nm) slowly forms a yellow-green product, supposedly a result of chlorine substitution by hydroxyl. This reaction occurs more rapidly in an alkaline medium (Figure 1a and Table S3); a similar process was observed for a Cl-containing heptamethine carbocyanine IR-783 [32]. During this color transition, the absorbance spectra (Figure 1b) show a slow decrease in intensity at 780 and 716 nm and an increase at 450 nm.

3.2. Reaction of Hypochlorite with Dye I

When reacted with millimolar concentrations of NaOCl in acidic and neutral media (pH < 9; Table S3), dye I instantly and reversibly forms a dark-violet product I (λ_{max}= 520, 560, and 600 nm, Figure 1d; Scheme 1), presumably an adduct (when formed on mixing of reactants, product I can disappear in seconds to yield other products). In an alkaline medium (pH > 9), colorless or yellow products are rapidly formed instead of product I. In glycine buffer (pH 9), however, hypochlorite has no effect; rather, a grass-green product is developed, presumably due to the substitution of chlorine by the glycine moiety. It is likely that the light-green colored products are formed as a result of chlorine substitution with OH or a nucleophilic analyte, and this group of products is denoted as product II

(Scheme 1). At a lower pH, discoloration occurs but more slowly; at pH 5.6 used in this study, product I discolors in about 10 min (Figure 1d), which is a convenient time to follow the reaction in assays.

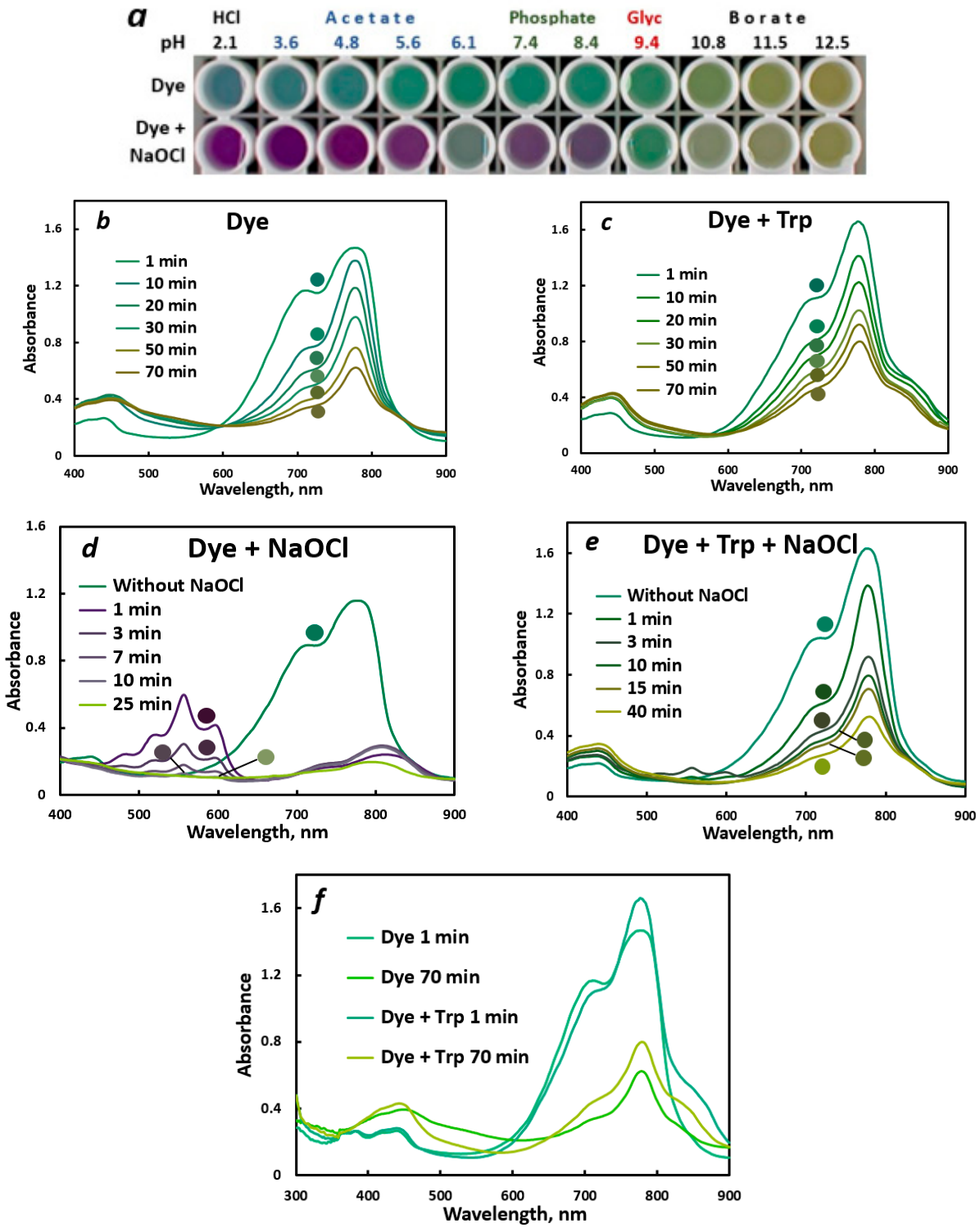

Figure 1. View of the plate with the reaction mixtures at various pH with and without NaOCl at 2 min reaction time (**a**). Absorbance spectra at pH 5.6: (**b**)—dye I; (**c**)—dye I + tryptophan; (**d**)—dye I + NaOCl; (**e**)—dye I + NaOCl + tryptophan (full system); (**f**)—excerpts from Figure (**b**,**c**) (dye alone and dye + trp). Concentrations in the cell: 0.01 g/L dye, 2.5×10^{-4} M NaOCl, 5×10^{-5} M trp. The nature of the buffer is shown above the pH value (Glyc: glycine buffer).

3.3. Interaction of Model Analytes with Dye I (Without NaOCl)

Nucleophilic analytes compete with hydroxyl to give chlorine substitution products of the dye. For example, tryptophan (trp) forms a grass-green product (type II) with a spectrum that is similar (but not identical) to that of the hydrolysis product (Figure 1c,f). However, screening of the analytes' interaction with dye I in a 96-well plate using an RGB camera did not reveal any noticeable color effects; retardation of the reaction is only observed for several analytes (DNA, BSA, succinate, the three surfactants, and ascorbate). This may be explained by the fact that the two green compounds, the parent dye and product II, are similarly colored. Amino compounds do not give any visible effect in this system (the PCA scores plot is shown in Figure S1 in the ESI together with an image of the plate). Due to lacking contrast, this process is not used as an indicator reaction.

3.4. Effect of Model Analytes in the Carbocyanine–NaOCl Reaction

The situation changes in the presence of NaOCl due to a distinctly colored product I that is formed in the blank run. In the presence of a highly reactive analyte (tryptophan), the absorbance at 780 nm decreases; a small amount of product I is seen at 3 min at 520–600 nm, but it vanishes in a few minutes, and the grass-green substitution product II is formed (Figure 1e).

The effects of the model analytes studied under the screening conditions in a 96-well plate are shown in Figure 2a. Strong reducing agents (ascorbate, cysteine) prevent NaOCl from reacting with the dye, which preserves the emerald-green color of the solution for a long time. Other compounds slow down the discoloring of violet product I: amino acids (serine, leucine, glutamine, alanine), amines (methylamine, diethylamine), urea, and O-compounds (succinate, oxalate, acetaldehyde), as well as NH_4^+, $Ca^{2+,}$ and Mg^{2+}. Tryptophan forms the grass-green product II. Dodecyl sulfate (SDS) gives a uniquely colored product, Triton X-100 causes fast bleaching, while CTAB has a little effect. Small molecules (isopropanol, acetaldehyde and acetone, citrate) and sugars demonstrate weak effects in this reaction. In general, the most diverse influence of the model analytes is observed in the dye–NaOCl system, which is manifested in the formation of products of different colors at different reaction times.

The described color effects refer to the Millipore water medium. When an aliquot of natural (borehole) water is added to the reaction mixture, the indicator reaction is accelerated (Figure 2b). Ascorbate and cysteine are most active, similarly to the Millipore water medium, but besides them, the emerald-green color of the initial dye is also preserved during the first 5 min of the reaction by tryptophan, BSA, and phenol. DNA also has a stronger effect than in Millipore water, yielding a green product. Carboxylates (amino acids, oxalate, and succinate) slow down the formation of violet product I and its bleaching; the same behavior is observed for both amines, both amides (urea and creatinine), $NH_4^{+,}$ and Mg^{2+}. The effects of surfactants are essentially the same as in Millipore water.

The observed complex pattern of color transitions (Figure 2) can be understood by taking into account multiple effects of the analytes: (1) slowing down the disappearance of the emerald-green initial dye color, most likely by direct reaction with hypochlorite; (2) slowing down the discoloration of the deep-violet product I, the putative adduct of HOCl with the dye; and (3) formation of the grass-green products of type II, candidate products of the substitution of chlorine in the dye. Process (1) is due to reducing agents; process (2) is presumably due to chlorine radical scavenging, and this is the most "popular" mechanism of action among the model analytes studied. Process (3) occurs more rapidly with selected nucleophiles such as phenolate and tryptophan; it can also occur with nucleophilic primary amines and amino acids, but the resulting products may have no distinct spectral differences compared to the control. Substitution of chlorine (3) is supposed to compete with hydrolysis, both yielding similarly colored grass-green or yellow-green products. Moreover, it is very likely that substitution (3) competes with the oxidation of the dye by hypochlorite to give the violet product I; this can be noticed in the presence of phenol in the Millipore water medium (Figure 2a), where the violet product I is replaced by the green product II. This

fact confirms the reversibility of product I formation and supports the hypothesis that it is an adduct of the dye and hypochlorite.

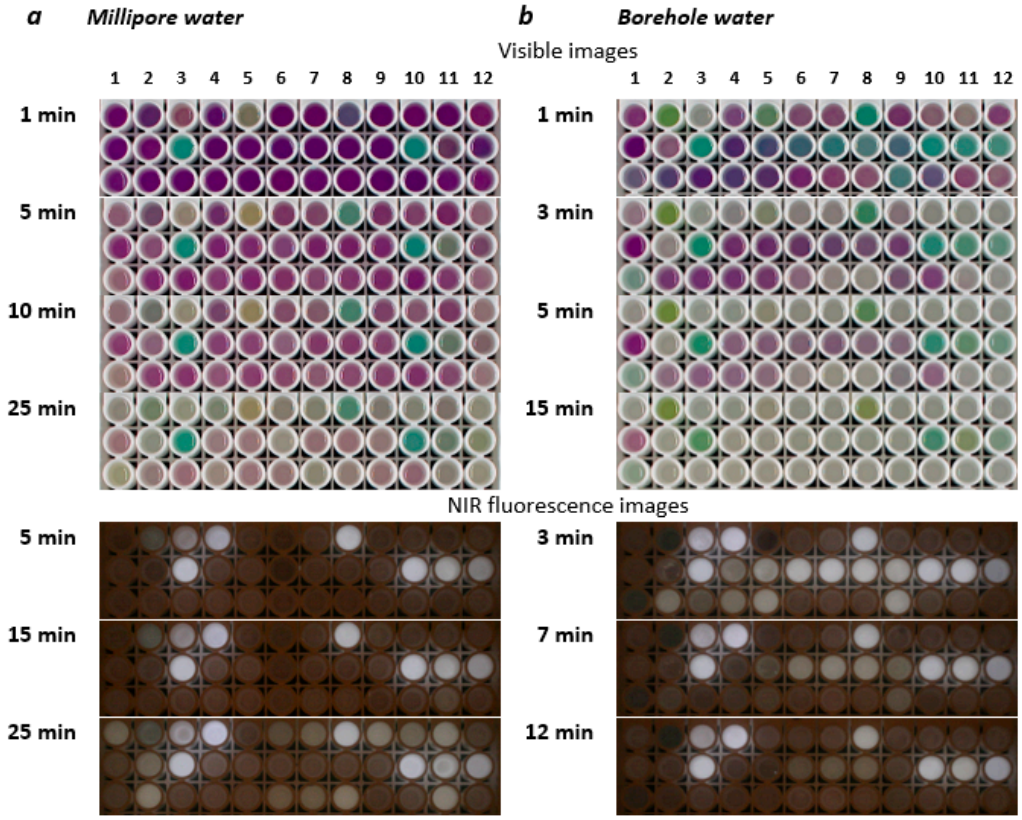

Figure 2. Images of the 96-well plate with the reaction mixtures of dye I with NaOCl in the presence of model compounds in Millipore water (**a**) and borehole water (**b**) taken at different times after adding the dye. Concentrations in the final reaction mixture: NaOCl 0.25 mM, dye I, acetate buffer (pH 5.6) 10 mM, model organic analytes 0.5 mM, inorganic compounds 1 mM, Cu and Co 0.1 mM, BSA 0.3 g/L, DNA 0.025 g/L. Model analytes, 1st row: control, 4-nitrophenol, Triton X-100, CTAB, SDS, fructose, glucose, phenol, isopropanol, acetone, acetaldehyde, control; 2nd row: succinate, oxalate, ascorbate, citrate, serine, glutamate, leucine, glutamine, alanine, cysteine, tryptophan, BSA; 3rd row: DNA, diethylamine, methylamine, creatinine, urea, $CaCl_2$, $NaNO_3$, KCl, $MgCl_2$, $(NH_4)_2SO_4$, $CuSO_4$, $CoSO_4$.

The difference between Millipore and natural water is the content of salts and organic matter, which can both influence the reaction rate and modify the effects of model analytes. Organic components of water can interact with the intermediate particles formed in the course of a radical oxidation reaction [33], as can redox-active metal ions such as $Fe^{(2+}$, $^{3+)}$ or Cu^{2+}. A rich content of dissolved organic matter in the samples opens up ample opportunities for such effects. The result is the different patterns of water matrix effects for the two types of water.

To compress the data obtained as color images, PCA score plots were constructed (Figure 3a,b). Without the addition of natural water, the most reactive compounds are displayed as points located far from the control (Figure 3a); other model analytes densely populate the area around the control and can hardly be discriminated. A more diverse picture is observed in the presence of natural water (Figure 3b): additional groups of moderately reactive amino acids (alanine, glutamate, glutamine, leucine) and less reactive nitrogen compounds (creatinine, urea, methylamine, serine, diethylamine) are separated in the score plot. Oxygen-containing compounds and inorganic salts represent a group around the control. Thus, natural water increased the diversity of the model analyte signals.

To obtain a more refined pattern of the model analytes' action, LDA score plots were constructed based on six replicate runs for each analyte (Figure 3c,d) using the RGB data obtained from the 96-well plate images. The reaction was conducted with 36 analytes and monitored for 40 min, during which 12 photographs were captured. The results show that the eight most reactive analytes (tryptophan, phenol, BSA, ascorbate, cysteine, DNA, methylamine, and SDS) are discriminated from each other and from a large group of less reactive compounds (Figure 3c). When the most reactive analytes were excluded from LDA processing, the less reactive compounds could be further subdivided into groups (Figure 3d). It is remarkable that eight nitrogen species (amines, amides, and amino acids) form an independent group, the organo-oxygen analytes and inorganic salts are clustered around the blanks, while the inorganic ammonium ion occupies an intermediate position. 4-Nitrophenol is discriminated mostly due to its intrinsic color.

Therefore, the reaction of dye I with hypochlorite can be used to discriminate between the compounds of different groups in natural water. The implication of these results is the feasibility of detecting and revealing the probable nature of a predominant contaminant. (The influence of one analyte on the signal of another is discussed in the following sections). Of particular interest are nitrogen-containing compounds as potential precursors of disinfection by-products. In this work, most of the further experiments with model analytes were conducted in the presence of a natural (borehole) water matrix.

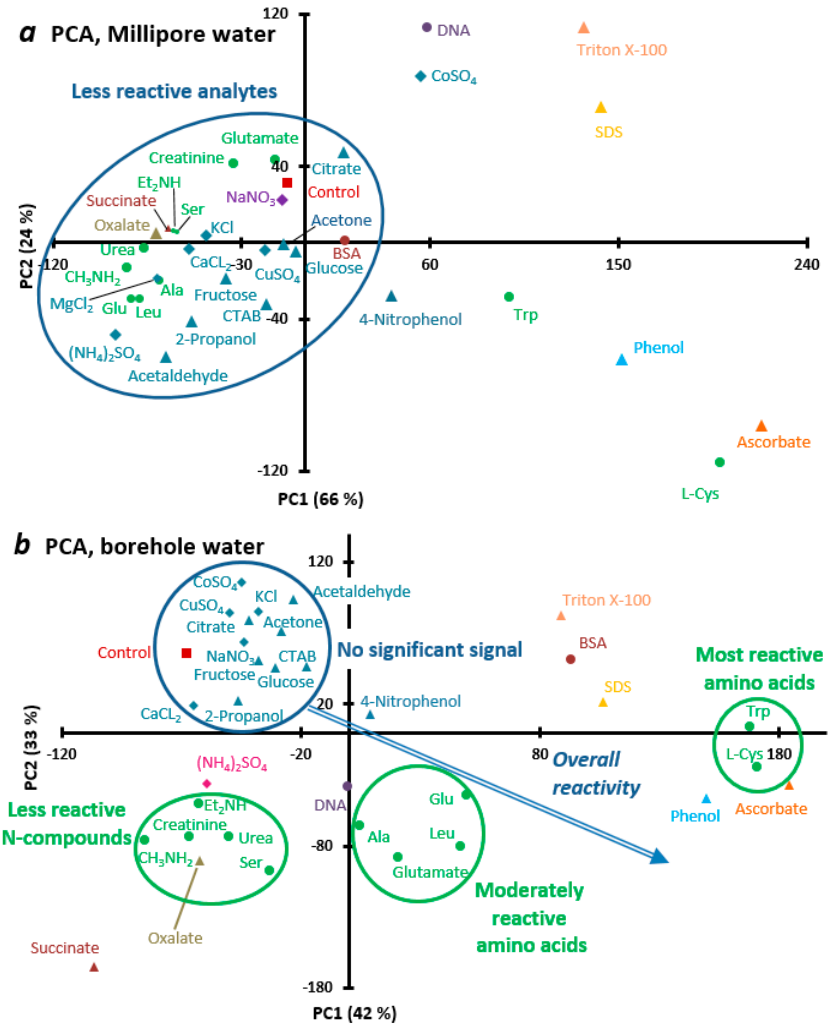

Figure 3. *Cont.*

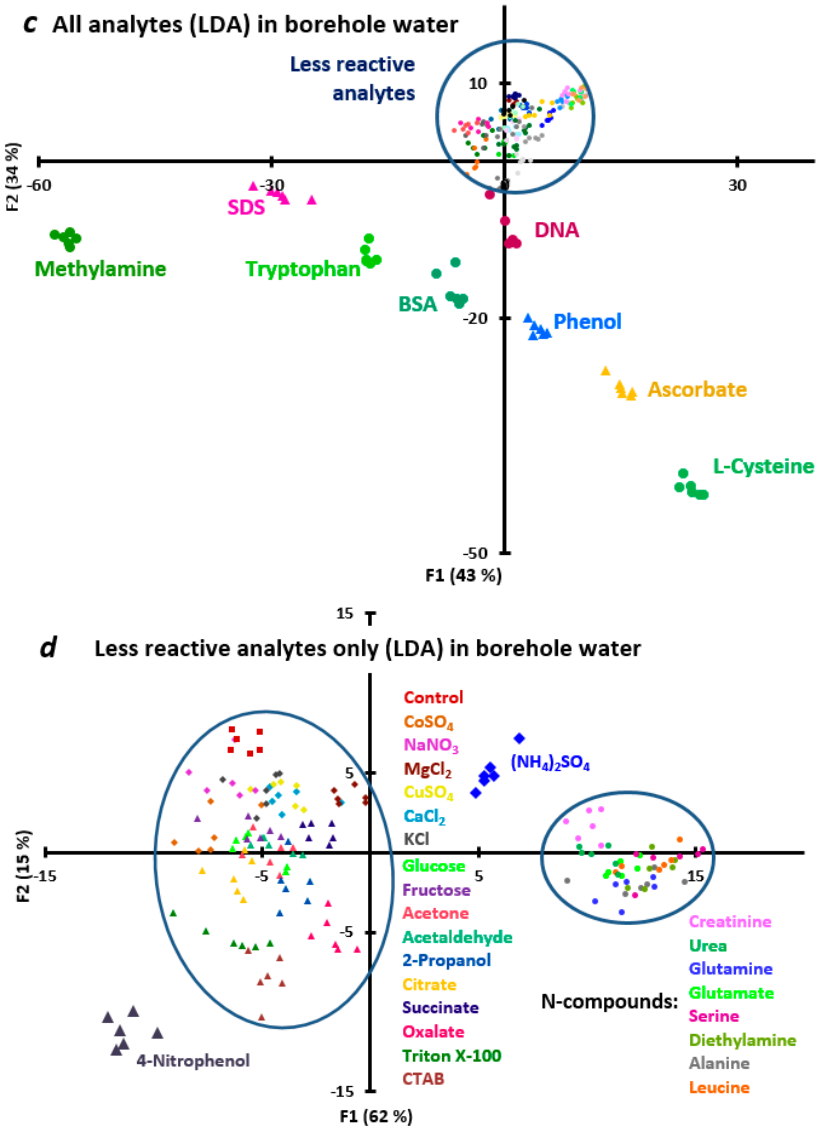

Figure 3. (**a**,**b**)—PCA score plots for the reaction mixtures containing dye I, NaOCl, buffer (pH 5.6), and a model analyte: (**a**)—in Millipore water, (**b**)—in borehole water (120 µL in the well); (**c**,**d**)—LDA score plots for the same reaction with six parallel runs for each model analyte in borehole water: (**c**)—all data were processed, (**d**)—only the group of less reactive compounds was processed.

3.5. Near-IR Signal Induced by Model Analytes

Carbocyanine dye I is fluorescent in visible (440 nm) and near-IR (800 nm) spectral regions. The NIR emission maximum is of greater analytical significance in the studied system than visible fluorescence, since its change is associated with polymethine chain destruction. However, the sensitivity of standard spectrofluorimeters to wavelengths higher than 800 nm is low (the spectra are given in Figure S2), and the dye signal can be confidently measured only using an NIR photo camera, which is more sensitive in this spectral region.

No enhancement in the fluorescence of the dyes was observed with any of the model compounds without added oxidant (a slight enhancement was observed with surfactants due to the increased quantum yield in premicellar structures). After adding NaOCl to the dye, the NIR signal instantly disappears in the control run, but some model analytes can maintain the signal (Figure 2), which may be due to the original dye remaining in the reaction mixture or the formation of reaction products with an intact polymethine chain. The trends in Millipore water and natural water are different: in the first medium,

some model analytes lead to an increase in intensity (Figure 2a), whereas in borehole water, some other analytes cause a reappearance of the NIR signal (Figure 2b). The set of analytes contributing to the NIR fluorescence intensity is different from the set of analytes contributing to the color change (Figure 2). Theoretically, NIR fluorescence could be used as an analytical signal; however, adding the fluorescence data to the RGB absorbance data for PCA processing showed but a little effect on the score plots. Further in this work, we relied only on the absorbance color channels as carrying most of the key information.

3.6. Dependence of the RGB Signal on the Concentration of Analytes

The concentration effects of the model analytes in borehole water were studied using tryptophan, BSA, and cysteine as more reactive analytes, and ethylamine, urea, and humic acids as less reactive ones. Reactive analytes at concentrations of $\geq 5 \times 10^{-5}$ M demonstrate a distinctly green color in the first minutes of the reaction, which is mostly due to the presence of the initial dye, while at $\leq 5 \times 10^{-6}$ M, the violet product I is formed (Figure 4). Analytes belonging to the less reactive group only show different intensities of violet color at high concentrations. At longer reaction times, grass-green substitution products (type II) can be observed for the reactive analytes; otherwise, the reaction mixture decolorizes. Emerald-green initial dye is only maintained in the presence of high amounts of cysteine (5×10^{-4} mM). Overall, individual analytes can be detected at the following concentrations in the well of the plate: tryptophan—5×10^{-8} M (at 1 min), cysteine—5×10^{-6} M (at 2 min), diethylamine—1×10^{-6} M (at 1–5 min), and urea—5×10^{-5} M (at 1 min), while humates yield no signal besides an intrinsic yellow color. All the mentioned results refer to the higher concentration of NaOCl (right column); at a lower concentration (1.4×10^{-4} M), humates are detectable at the time of 15 min; otherwise, the detection limits are the same or higher than those with the higher NaOCl concentration.

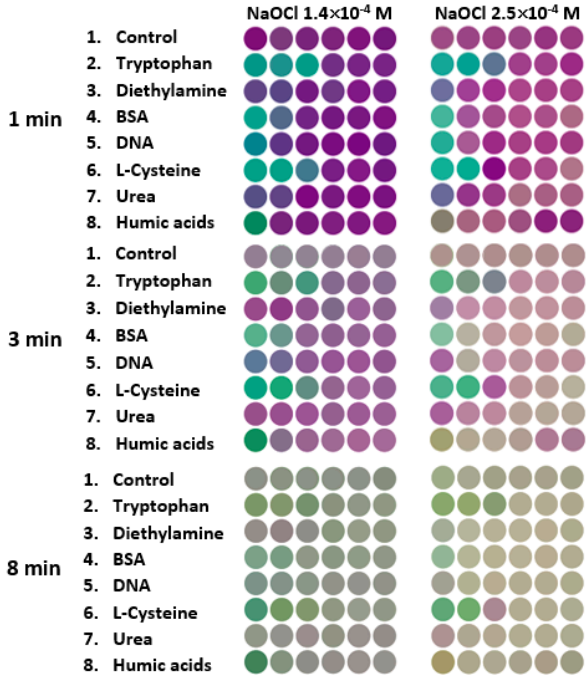

Figure 4. Effect of concentration of nitrogen compounds (rows 2–8) on the colorimetric signal in the *dye–NaOCl* reaction for two concentrations of NaOCl (shown above the left and right columns) in borehole water. The colors were averaged over the well of the plate. Rows correspond to different analytes; the concentration of each analyte increases from left to right by an order of magnitude (1—control): 2—tryptophan, from 0.5 mM to 50 nM; 3—diethylamine, 0.1 mM to 10 nM; 4—BSA, 0.03 g/L to 3 μg/L; 5—L-cysteine, 0.5 mM to 50 nM; 6—urea, 0.5 mM to 50 nM; 7—humic acids, 0.023 g/L to 2.3 μg/L. All concentrations refer to the reaction mixtures in the plate.

The results described above refer to the borehole water. The natural water matrix increases the detection limits of analytes, which can be illustrated by the example of amino acids that have 1–2 orders of magnitude higher LODs in the natural water (Table 1). This trend is emphasized since selectivity, on the contrary, is more favorable in well water (compare Figure 3a,b).

Table 1. Limits of detection of amino acids (µmol/L) in Millipore and borehole water.

Amino Acid	Millipore	Borehole
Glutamate	0.05	5
Glycine	0.05	5
Alanine	0.5	5
Serine	0.5	5
Leucine	0.5	5
Cysteine	5	50

Notes. The concentration values refer to the wells of the plate. The LODs were estimated to an order of magnitude using LDA score plots constructed from reaction kinetics.

3.7. Effects of Analytes in Mixtures

As can be seen from the above, the high concentrations of most reactive analytes can be visually detected in the first minutes of the reaction by the green color of the solution. Investigation of whether other nitrogen-containing compounds affected this signal (mutual influence of analytes) was performed using tryptophan as the analyte in the presence of added urea and BSA. As these compounds are less reactive than trp, little interference on the signal of trp was expected. For the mixtures of trp + urea (or trp + BSA), the color changes were observed (the images of the 96-well plates at different reaction times are given in Table S4 in ESI). To describe the color effects for all reaction times and convolve the data, LDA score plots were constructed (Figure 5). It can be seen that the 5×10^{-4} M and 5×10^{-5} M concentrations of trp are well discriminated with and without urea; 5×10^{-6} M trp takes an intermediate position without urea but combines with the group of blank images in the presence of urea, which implies that at this concentration, urea interferes with the detection of trp. Overall, urea does not demonstrate strong influence on trp detection (Figure 5a).

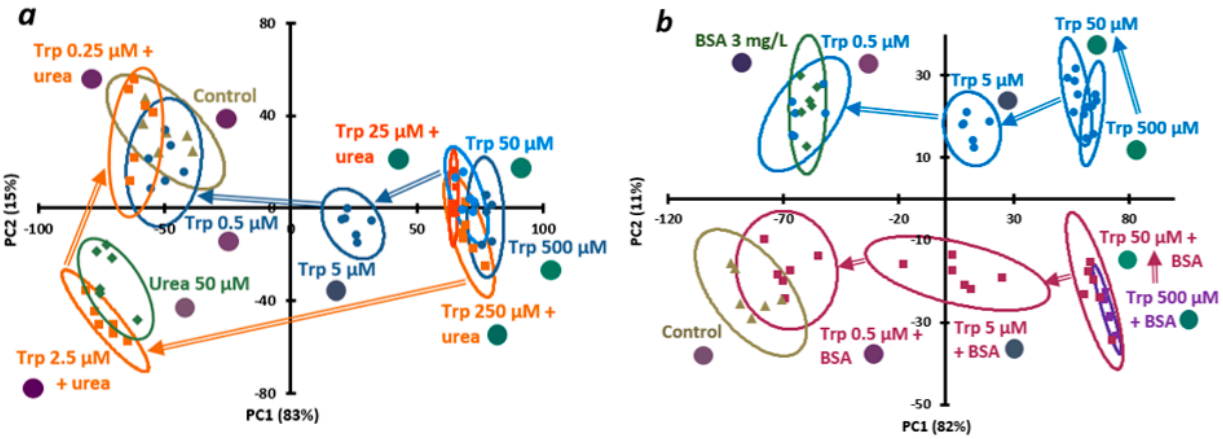

Figure 5. PCA score plots for the reaction *dye I–NaOCl* with various amounts of tryptophan: (**a**)—in the presence of 5×10^{-5} M urea; (**b**)—in the presence of 3 mg/L BSA. The photographs of the reaction mixtures were captured at 1, 2, 3, and 5 min after mixing the reactants (Table S4); each experiment was run in six replicates (six points in the graphs). Actual color of the wells at 1 min after mixing the reactants is shown beside the group of the corresponding points as large circles. All concentrations are final (in the well).

A more reactive analyte (BSA) was similarly investigated in the mixture with trp (Figure 5b). In this case, color changes over time in the presence of 5×10^{-6}–5×10^{-7} M trp and a constant amount of BSA differ from those with urea (Table S4 and color circles in Figure 5b); however, the main trends of the color changes with the concentration of tryptophan are similar with and without BSA. The minimum detectable concentration of trp alone and with BSA is the same (5×10^{-7} M). Therefore, introduction of an additional model compound (urea, protein) into the system does not eliminate the concentration effect of tryptophan. These results confirm the high discriminative ability of the proposed reaction with respect to some nitrogen-containing analytes.

3.8. Effect of the Time Interval Between Adding Hypochlorite and the Dye

The aim of this experiment was to evaluate the possibility of detecting chlorination products after treating water with active halogen-containing disinfectants. To simulate water chlorination in a wastewater treatment plant and the subsequent visualization of its products, we prepared the reaction mixtures but without the dye (model analyte + buffer + NaOCl); dye addition was delayed for 1 to 24 h, after which the reaction was followed in a regular way. Four model compounds were tested in this way (Tables 2 and S5). Without a delay before adding the dye, DNA, BSA, and lysozyme were detected, but at long reaction times (from 5 min and on). After a delay of 1 h, BSA showed the same activity, while DNA became noticeable already in the first minutes of the reaction; lysozyme was virtually undetectable. Unexpectedly, after a delay time of 24 h, only lysozyme gave the signal, but starting from the first minutes of the reaction. The reactivity of the mixture several hours after the addition of NaOCl can be associated mainly with the formation of chloramines and similar products that themselves serve as oxidants. The behavior of the model analytes (Tables 2 and S5) reflects the complex chemistry of the chlorination products and confirms that such products can exist in water for up to 24 h, remaining reactive towards the carbocyanine dye, and can be visualized using this reaction. In this experiment, the concentrations were high to reveal the main features of the system; in real water samples, they will be lower, but it will still be possible to obtain signals of reactive compounds down to at least 0.5 mg/L, as shown in Section 3.4. Overall, the indicator reaction is promising for mimicking the chlorination processes with the subsequent visualization of the stable chlorination products.

Table 2. Model analytes that can be visualized in water at different delay times.

Delay Time *, h	Model Analyte (Time of Developing the Signal After Reaction Start)
0	DNA (5–40 min), BSA (15–40 min), lysozyme (30–40 min)
1	DNA (1–40 min), BSA (15–40 min)
24	Lysozyme (1–40 min)

* Time between adding the dye to the mixture of NaOCl and analyte.

3.9. Testing of Wastewater and Natural Water Samples

Three sewage and three natural water samples were added to the *NaOCl–dye* system. Wastewater samples were completely discriminated by LDA from the natural waters and controls: samples WW-1 and WW-4 prevented the formation of dark-purple product I (the reaction mixture remained green), while WW-7 slowed down product I formation (the colors are shown in the LDA score plot, Figure 6a). The strongest effect was observed for the two wastewaters with the highest permanganate index, i.e., the total reducing compounds (characteristics of the samples are given in Table S6).

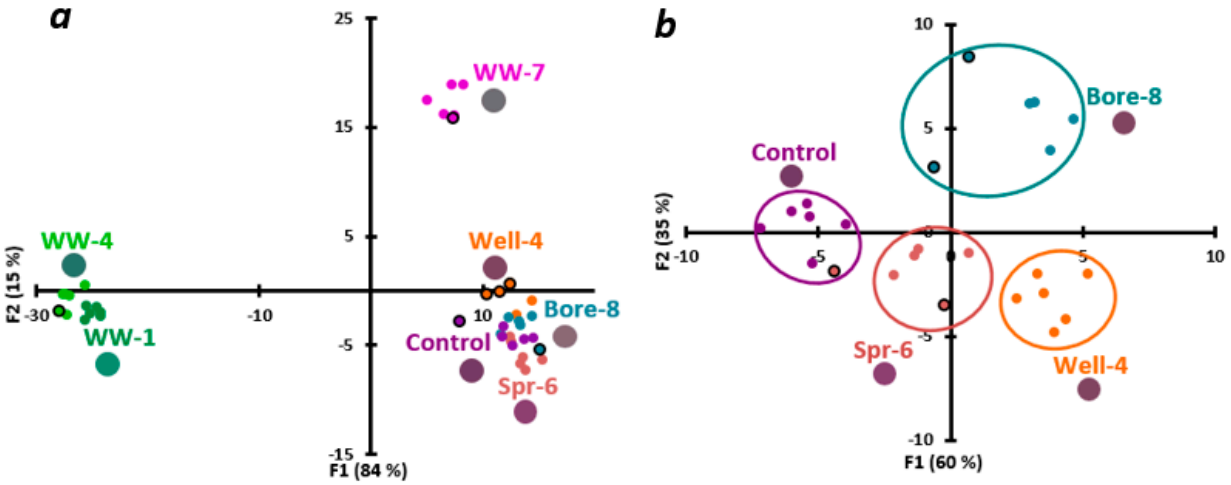

Figure 6. LDA score plots for the indicator reaction *dye I–NaOCl* with added natural water (Spring-6, Well-4, Borehole-8) and wastewater (WW) samples. The color of the wells on the third min of reaction is shown as a large circle beside the corresponding group of points. (**a**)—data for all six samples were processed; (**b**)—only three natural water samples and control were processed. Validation observations are shown as dots with the same color and a black border.

The natural water samples behaved similarly to the controls, but slight differences were still observed in the rate of disappearance of the violet color and acquisition of grass-green color at a long reaction time (25 min). In the LDA score plot, the three natural water samples formed one group (Figure 6a), but when processed without the wastewater samples, the natural waters were partially discriminated (Figure 6b; accuracy 75%). Thus, the proposed indicator reaction is capable of discriminating heavily polluted water (such as wastewater) and natural water and can partly discriminate samples within these water types. In the future, it will be possible to identify predominant reactive analytes in wastewater, provided that the study of the main water components has been undertaken by alternative methods.

4. Conclusions

In this study, we propose a reaction of carbocyanine oxidation with hypochlorite that yields differently colored products for obtaining the signal from the reactive compounds: amines and amino acids, proteins, DNA, phenols, and some others. The said compounds have been found to inhibit oxidation, which is accompanied by a color difference from the control run, allowing the observation of kinetic curves that are typical for groups of analytes. Detection is selective enough to discriminate the most reactive compounds from each other and from the less reactive ones, and nitrogen-containing organic compounds from other model analytes.

The advantages of the proposed system are as follows: contrast color change, which is different for groups of analytes acting by different mechanisms; possibility to measure the signal by capturing photographic images of the reaction mixture with a smartphone or using a visualizer, as well as perform visual detection; and feasibility to carry out detection in a natural water matrix. The process is rapid and simple and can be used as a foundation for the development of group assays in real-world samples. The strategy is not about determining individual components; on the contrary, the idea is to measure a signal from a large group of substances to obtain maximum information about the sample with a single test. Such simple methods can be realized outside the laboratory; for this purpose, ready-to-use dry assay systems in 96-well plates can be developed. All that remains to be performed is to add the water sample to the plate with all the necessary reagents and buffer in the wells, after which the detection can be carried out in the usual way.

This study is the first part of multi-stage research aimed at solving a challenging task of water quality monitoring by fingerprint techniques. The next steps are to compare

the signals obtained by the proposed and existing methods (e.g., HPLC-MS/MS) before moving on to real-world applications; this work will classify the sample types and identify their distinguishing features. As a result, the range of analytes and types of samples will be expanded.

In addition to the screening of samples, the proposed indicator system may also allow for the quantitation of nucleophilic analytes, especially amino compounds. Another potential of the proposed system is the detection of chlorinated products immediately after water treatment with chlorine or NaOCl, the products of which are oxidants capable of reacting with the chromogenic dye. The work can be successful only if machine learning methods are adequately used.

Supplementary Materials: The following supporting information can be downloaded at: https://www.mdpi.com/article/10.3390/chemosensors12110224/s1, spectral data for dye I; Table S1: Composition of natural water samples; Table S2: Inorganic components of natural water samples according to total reflectance X-ray fluorescence (TXRF)* (mg/L); Table S3: Effect of pH on the color of the reaction system; Table S4: Images of the wells for selected reaction times. Table S5: Images of the wells with four model analytes in dye I–NaOCl reaction started at different times after adding NaOCl; Table S6: Concentration of nitrogen species and chemical oxygen demand in water samples; Figure S1: PCA score plot for mixtures of dye I with model analytes without NaOCl; Figure S2: fluorescence spectra of dye I and its reaction products with NaOCl.

Author Contributions: Conceptualization, M.K.B.; data curation, R.M.A.; methodology, T.A.P. and M.K.B.; investigation, A.V.S., E.V.S. and I.A.D.; writing—original draft preparation, A.V.S. and G.K.S.; writing—review and editing, M.K.B.; resources, I.A.D. and T.A.P.; software, R.M.A.; funding acquisition, G.K.S. All authors have read and agreed to the published version of the manuscript.

Funding: The article was prepared within the project "The "Clean Water" project as the most important component of cooperation between the Russian Federation and the countries of the Global South: socio-economic and technological dimensions" supported by the grant from the Ministry of Science and Higher Education of the Russian Federation program for research projects in priority areas of scientific and technological development (Agreement No 075-15-2024-546).

Institutional Review Board Statement: Not applicable.

Informed Consent Statement: Not applicable.

Data Availability Statement: All data necessary to reproduce our results are presented in the main text and in the electronic Supporting information. Raw data are available upon request.

Acknowledgments: The authors express their gratitude to the Analytical Center of Moscow University and personally to Alexander D. Smolenkov and Olga G. Tataurova for providing water samples and results of their analysis.

Conflicts of Interest: The authors declare no conflicts of interest. The funder had no role in the design of the study; in the collection, analyses, or interpretation of data; in the writing of the manuscript, or in the decision to publish the results.

References

1. The United Nations World Water Development Report 2024: Water for Prosperity and Peace. UNESCO. 2024. Available online: https://unesdoc.unesco.org/ark:/48223/pf0000388948 (accessed on 28 August 2024).
2. Repeta, D.J. Chapter 2—Chemical Characterization and Cycling of Dissolved Organic Matter. In *Biogeochemistry of Marine Dissolved Organic Matter*, 2nd ed.; Hansell, D.A., Carlson, C.A., Eds.; Academic Press: Cambridge, MA, USA, 2015; pp. 21–63. [CrossRef]
3. Shi, W.; Zhuang, W.-E.; Hur, J.; Yang, L. Monitoring dissolved organic matter in wastewater and drinking water treatments using spectroscopic analysis and ultra-high resolution mass spectrometry. *Water Res.* **2021**, *188*, 116406. [CrossRef] [PubMed]
4. Chen, W.; Yu, H.-Q. Advances in the characterization and monitoring of natural organic matter using spectroscopic approaches. *Water Res.* **2021**, *190*, 116759. [CrossRef] [PubMed]
5. Xu, X.; Thomson, N.R. Estimation of the maximum consumption of permanganate by aquifer solids using a modified chemical oxygen demand test. *J. Environ. Eng.* **2008**, *134*, 353–361. [CrossRef]
6. Stauß, A.C.; Fuchs, C.; Jansen, P.; Repert, S.; Alcock, K.; Ludewig, S.; Rozhon, W. The Ninhydrin Reaction Revisited: Optimisation and Application for Quantification of Free Amino Acids. *Molecules* **2024**, *29*, 3262. [CrossRef]

7. Aguilar Diaz de Leon, J.; Borges, C.R. Evaluation of Oxidative Stress in Biological Samples Using the Thiobarbituric Acid Reactive Substances Assay. *J. Vis. Exp.* **2020**, *159*, e61122. [CrossRef]
8. Chan, K.-Y.; Wasserman, B.P. Direct colorimetric assay of free thiol groups and disulfide bonds in suspensions of solubilized and particulate cereal proteins. *Cereal Chem.* **1993**, *70*, 22–26.
9. Apak, R.; Çekiç, S.D.; Üzer, A.; Çapanoğlu, E.; Çelik, S.E.; Bener, M.; Can, Z.; Durmazel, S. Colorimetric sensors and nanoprobes for characterizing antioxidant and energetic substances. *Anal. Methods* **2020**, *12*, 5266. [CrossRef]
10. Kumar, S.; Chaitanya, R.K.; Preedy, V.R. Chapter 20—Assessment of Antioxidant Potential of Dietary Components. In *HIV/AIDS*; Preedy, V.R., Watson, R.R., Eds.; Academic Press: Cambridge, MA, USA, 2018; pp. 239–253. [CrossRef]
11. Fernandes, G.M.; Silva, W.R.; Barreto, D.N.; Lamarca, R.S.; Gomes, P.C.F.L.; da S Petruci, J.F.; Batista, A.D. Novel approaches for colorimetric measurements in analytical chemistry—A review. *Anal. Chim. Acta* **2020**, *1135*, 187–203. [CrossRef]
12. Ali, R.B.; Omrani, R.; Akacha, A.B.; Dziri, C.; El May, M.V. Development and validation of a colorimetric method for the quantitative analysis of thioamide derivatives. *Spectr. Acta A* **2019**, *220*, 117154. [CrossRef]
13. Li, Z.; Suslick, K.S. The Optoelectronic Nose. *Acc. Chem. Res.* **2021**, *54*, 950–960. [CrossRef]
14. Yaroshenko, I.; Kirsanov, D.; Marjanovic, M.; Lieberzeit, P.A.; Korostynska, O.; Mason, A.; Frau, I.; Legin, A. Real-Time Water Quality Monitoring with Chemical Sensors. *Sensors* **2020**, *20*, 3432. [CrossRef] [PubMed]
15. Vaughan, A.A.; Narayanaswamy, R. Optical fibre reflectance sensors for the detection of heavy metal ions based on immobilised Br-PADAP. *Sens. Actuators B* **1998**, *51*, 368–376. [CrossRef]
16. Sasaki, Y.; Lyu, X.; Minami, T. Printed colorimetric chemosensor array on a 96-microwell paper substrate for metal ions in river water. *Front. Chem.* **2023**, *11*, 1134752. [CrossRef] [PubMed]
17. Ghohestani, E.; Tashkhourian, J.; Sharifi, H.; Bojanowski, N.M.; Seehafer, K.; Smarsly, E.; Bunz, U.H.F.; Hemmateenejad, B. A poly (arylene ethynylene)-based microfluidic fluorescence sensor array for discrimination of polycyclic aromatic hydrocarbons. *Analyst* **2022**, *147*, 4266–4274. [CrossRef]
18. Sicard, C.; Glen, C.; Aubie, B.; Wallace, D.; Jahanshahi-Anbuhi, S.; Pennings, K.; Daigger, G.T.; Pelton, R.; Brennan, J.D.; Filipe, C.D.M. Tools for water quality monitoring and mapping using paper-based sensors and cell phones. *Water Res.* **2015**, *70*, 360–369. [CrossRef]
19. Yang, M.; Zhang, M.; Jia, M. Optical sensor arrays for the detection and discrimination of natural products. *Nat. Prod. Rep.* **2023**, *40*, 628–645. [CrossRef]
20. Dickenson, E.R.V.; Snyder, S.A.; Sedlak, D.L.; Drewes, J.E. Indicator compounds for assessment of wastewater effluent contributions to flow and water quality. *Water Res.* **2011**, *45*, 1199–1212. [CrossRef]
21. Harwood, J.J. Molecular markers for identifying municipal, domestic and agricultural sources of organic matter in natural waters. *Chemosphere* **2014**, *95*, 3–8. [CrossRef]
22. Sirivedhin, T.; Gray, K.A. Part I. Identifying anthropogenic markers in surface waters influenced by treated effluents: A tool in potable water reuse. *Water Res.* **2005**, *39*, 1154–1164. [CrossRef]
23. Chen, H.; Xie, J.; Huang, C.; Liang, Y.; Zhang, Y.; Zhao, X.; Ling, Y.; Wang, L.; Zheng, Q.; Yang, X. Database and review of disinfection by-products since 1974: Constituent elements, molecular weights, and structures. *J. Hazard. Mater.* **2024**, *462*, 132792. [CrossRef]
24. Mazur, D.M.; Lebedev, A.T. Transformation of Organic Compounds during Water Chlorination/Bromination: Formation Pathways for Disinfection By-Products (A Review). *J. Anal. Chem.* **2022**, *77*, 1705–1728. [CrossRef]
25. Shen, Y. Formation of nitrogenous disinfection by-products (N-DBPs) in drinking water: Emerging concerns and current issue. *IOP Conf. Ser. Earth Environ. Sci.* **2021**, *801*, 012015. [CrossRef]
26. Unprecedented Flooding Displaces Hundreds of Thousands Across East Africa. UN News. Available online: https://news.un.org/en/story/2024/05/1149461 (accessed on 28 August 2024).
27. Skorobogatov, E.V.; Shik, A.V.; Sobolev, P.V.; Stepanova, I.A.; Orekhov, V.S.; Ustyuzhanin, A.O.; Koksharova, M.V.; Ikhalaynen, Y.A.; Timchenko, Y.V.; Rodin, I.A.; et al. Monitoring Different Water Types for Engine Oil Water-Soluble Fraction and Iron(2+) Using a Reaction-Based Optical Sensing Strategy: A Proof-of-Concept Study. *Ind. Eng. Chem. Res.* **2024**, *63*, 12336–12349. [CrossRef]
28. Skorobogatov, E.V.; Timchenko, Y.V.; Doroshenko, I.A.; Podrugina, T.A.; Rodin, I.A.; Beklemishev, M.K. Determination of Isoniazid by a Photometric Method due to Covalent Binding with a Carbocyanine Dye. *J. Analyt. Chem.* **2024**, *79*, 417–425. [CrossRef]
29. Doroshenko, I.A.; Aminulla, K.G.; Azev, V.N.; Kulinich, T.M.; Vasilichin, V.A.; Shtil, A.A.; Podrugina, T.A. Synthesis of modified conformationally fixed tricarbocyanine dyes for conjugation with therapeutic agents. *Mendeleev Commun.* **2021**, *3*, 615–621. [CrossRef]
30. Zakharenkova, S.A.; Katkova, E.A.; Doroshenko, I.A.; Kriveleva, A.S.; Lebedeva, A.N.; Vidinchuk, T.A.; Shik, A.V.; Abramchuk, S.S.; Podrugina, T.A.; Beklemishev, M.K. Aggregation-based fluorescence amplification strategy: "turn-on" sensing of aminoglycosides using near-IR carbocyanine dyes and pre-micellar surfactants. *Spectrochim. Acta A* **2021**, *247*, 119109. [CrossRef]
31. Redmon, J.; Divvala, S.; Girshick, R.; Farhadi, A. Just Watch Once: Unified Real-Time Object Detection. In Proceedings of the IEEE Conference on Computer Vision and Pattern Recognition, Las Vegas, NV, USA, 27–30 June 2016; pp. 779–788. [CrossRef]

32. Stepanova, I.A.; Shik, A.V.; Skorobogatov, E.V.; Bartoshevich, A.A.; Beklemishev, M.K. Colorimetric determination of cetyltrimethylammonium bromide by using aggregation with a carbocyanine dye. *Anal. i Kontrol' [Anal. Control.]* **2022**, *26*, 204–211. [CrossRef]
33. Perez-Bendito, D.; Silva, M. *Kinetic Methods in Analytical Chemistry*; Ellis Horwood: New York, NY, USA, 1988.